11-1998

Dynamics of Biomolecules: Assignment of Local Motions by Fluorescence Anisotropy Decay

Carl N. Bialik

Barnabas Wolf

Edward L. Rachofsky

J. B. A. Ross
University of Montana - Missoula, sandy.ross@umontana.edu

William Laws
University of Montana - Missoula, bill.laws@umontana.edu

Dynamics of Biomolecules: Assignment of Local Motions by Fluorescence Anisotropy Decay

Carl N. Bialik, Barnabas Wolf, Edward L. Rachofsky, J. B. Alexander Ross, and William R. Laws
Department of Biochemistry, Mount Sinai School of Medicine, New York, New York 10029 USA

ABSTRACT Many biological systems have multiple fluorophores that experience multiple depolarizing motions, requiring multiple lifetimes and correlation times to define the fluorescence intensity and anisotropy decays, respectively. To simplify analyses, an assumption often made is that all fluorophores experience all depolarizing motions. However, this assumption usually is invalid, because each lifetime is not necessarily associated with each correlation time. To help establish the correct associations and recover accurate kinetic parameters, a general kinetic scheme that can examine all possible associations is presented. Using synthetic data sets, the ability of the scheme to discriminate among all nine association models possible for two lifetimes and two correlation times has been evaluated. Correct determination of the association model, and accurate recovery of the decay parameters, required the global analysis of related data sets. This general kinetic scheme was then used for global analyses of liver alcohol dehydrogenase anisotropy data sets. The results indicate that only one of the two tryptophan residues in each subunit is depolarized by process(es) independent of the enzyme's rotations. By applying the proper kinetic scheme and appropriate analysis procedures to time-resolved fluorescence anisotropy data, it is therefore possible to examine the dynamics of specific portions of a macromolecule in solution.

INTRODUCTION

Fluorescence spectroscopy provides a variety of methods to obtain information about the properties of biological macromolecules. For example, a change in a steady-state (time-averaged) fluorescence signal such as intensity or anisotropy (depolarization) can be used to follow a chemical reaction or an assembly interaction. In addition, the inherent sensitivity of fluorescence allows many biological systems to be examined at the physiological concentrations of the system components.

More detailed information can be determined through time-resolved fluorescence experiments. In particular, dynamic properties of the local environment of a fluorophore can be evaluated on the nanosecond time scale by examining the kinetics of the fluorescence intensity and anisotropy decays. Besides providing information on structural dynamics in the vicinity of a fluorophore, time-resolved fluorescence anisotropy can report on the hydrodynamic properties of a macromolecule or complex. In practice, this technique works well with molecules that are essentially spherical because only one rotational correlation time must be determined. Nonspherical macromolecules, however, have multiple correlation times that generally are difficult to resolve from fluorescence anisotropy decay data. For example, there are five possible correlation times for an ellipsoid, but only three are resolvable because two pairs of times are essentially degenerate (Small and Isenberg, 1977). If a fluorophore also experiences local depolarizing motions independent of the rotations taken by a macromolecule (of any shape), the data analysis problem is compounded further because even more correlation times must be resolved and interpreted. Aspects of these local motions have been investigated [c.f. treatments by Kinosita et al. (1982), Vogel and Jaehnig (1984), Restall et al. (1989), Stein et al. (1990), and van der Heide et al. (1993)]. As a result, while time-resolved fluorescence anisotropy has provided excellent information for a few biological systems, it has been used sparingly.

Resolving multiple correlation times is thus a fundamental issue in the analysis of fluorescence anisotropy decay data. The appropriate choice of a kinetic mechanism for both the intensity and anisotropy decay is a crucial factor in this analysis, and becomes particularly important when neither the intensity nor the anisotropy decays can be fit to a single exponential. When this situation occurs, each decay must be described by a more complex function; typically, sums of exponentials are used which are characterized by multiple fluorescence lifetimes and correlation times. Multiple intensity decay lifetimes are frequently observed with biomolecules for a variety of reasons. Two common scenarios are multiple fluorophores and heterogeneous environments for a single fluorophore. Causes for multiple correlation times were mentioned above. Thus, when a macromolecule contains multiple fluorophores and complex depolarizing motions are occurring, analysis of the time-resolved fluorescence anisotropy decay will require multiple lifetimes and correlation times.

Received for publication 30 March 1998 and in final form 14 July 1998.

Address reprint requests to Dr. William R. Laws, Department of Biochemistry, Mount Sinai School of Medicine, One Gustave L. Levy Place, New York, NY 10029. Tel.: 212-241-6545; Fax: 212-996-7214; E-mail: wlaws@smtplink.mssm.edu.

Preliminary accounts of this work have been presented at the 1997 Annual Meeting of the Biophysical Society (Bialik et al., 1997) and the 1998 International Biomedical Optics Symposium of SPIE (Bialik et al., 1998). It was also the basis of a submission by one of us (C.N.B.) to the 1997 Westinghouse Science Talent Search.

0006-3495/98/11/2564/10 $2.00

To simplify data analysis, it is often assumed that each fluorophore is subject to all of the depolarizing motions. This assumption means that each intensity decay lifetime is associated with each correlation time. Unfortunately, numerous biological systems exist where this assumption is invalid. For example, two fluorophores may reside in different environments within a macromolecule and, therefore, have different lifetimes. If only one fluorophore experiences local motion(s), only its lifetime should associate with the resulting short correlation time(s), while all fluorescence intensity lifetimes should associate with the correlation time(s) resulting from the rotation of the macromolecule.

To address this issue in data analysis, we present a general kinetic scheme that permits each of the possible associations between fluorescence intensity decay lifetimes and rotational correlation times to be evaluated individually. This development differs from a brief discussion presented by Brand et al. (1985), in that it is based on resolving the unique time-resolved fluorescence anisotropy decay of each individual fluorophore instead of determining an averaged set of parameters. To determine the utility of this approach, the ability to discriminate between the different association models for the simple case of two lifetimes and two correlation times has been tested. Unequivocal recovery of the correct associations between lifetime and correlation times was achieved for a series of synthetic data sets, provided that several related data sets sharing common parameters were analyzed simultaneously. The anisotropy decays of the two tryptophan residues per subunit of the homodimeric enzyme liver alcohol dehydrogenase (LADH) were also examined by this novel approach. Analysis of LADH anisotropy data sets by all of the two-lifetime, two-correlation time association models suggests that only one Trp residue experiences an independent depolarizing process. Thus, it becomes possible to assign a particular depolarization mechanism, such as a local motion within a macromolecule, to a specific fluorophore.

THEORY

Associations between lifetimes and correlation times

Consider a fluorophore which in solution has a single exponential intensity decay of lifetime τ. To evaluate its time-resolved fluorescence anisotropy by time-correlated single photon counting, decay curves are typically obtained at three angles of an emission polarizer using repeated excitations by a short pulse of vertically polarized light. At the magic angle (M), or 54.7° from the vertical (Azumi and McGlynn, 1962; Kalantar, 1968; Paoletti and LePecq, 1969; Shinitzky, 1972), the intensity decay, $I_M(t)$, represents the true intensity decay in that it is unaffected by depolarizing motions occurring during the lifetime of the excited state. The other two polarizer orientations are vertical (V), or parallel to the polarization of the exciting photons, and horizontal (H), or perpendicular. These two positions yield intensity decays $I_V(t)$ and $I_H(t)$, which differ from $I_M(t)$ as a result of the effect of depolarizing motions. The three decay functions are defined as

$$I_M(t) = \frac{\alpha}{3} e^{-t/\tau} \quad (1)$$

$$I_V(t) = I_M(t)\{1 + 2r(t)\} \quad (2)$$

$$I_H(t) = I_M(t)\{1 - r(t)\} \quad (3)$$

where α is a pre-exponential scaling term. The anisotropy decay of the fluorophore, $r(t)$, is given by

$$r(t) = \sum_{j=1}^{m} \beta_j e^{-t/\phi_j} \quad (4)$$

where there are m rotational correlation times, ϕ_j, that result from the depolarizing motions occurring during the lifetime of the excited state. The pre-exponential β_j terms represent the extent to which the emission is depolarized by each rotational component. For this simple fluorophore case, the individual β_j terms are functions of the excitation and emission dipoles of the fluorophore and the rotational diffusion coefficients of the molecule (Chuang and Eisenthal, 1972): $\beta_j \equiv f(\vec{\mu}_{ex}, \vec{\mu}_{em}, D_x, D_y, D_z)$. The correlation times, however, are functions of the rotational diffusion coefficients only: $\phi_j \equiv f(D_x, D_y, D_z)$. The sum of the β_j terms is the limiting anisotropy, r_0, which is determined by the angle between the excitation and emission dipoles of the fluorophore; thus r_0 is limited to a range of values: $-0.2 \leq r_0 \leq 0.4$. See Badea and Brand (1979), Lakowicz (1983), and the references within them for a more complete treatment.

Next, consider a heterogeneous sample with multiple emitting states. This sample could represent several possible physical systems, including a mixture of different fluorophores, multiple ground-state environments or conformations experienced by a single fluorophore, or multiple close-lying excited states of a single fluorophore. The intensity decay of such a heterogeneous sample is a sum of exponentials:

$$I_M(t) = \frac{1}{3} \sum_{i=1}^{n} \alpha_i e^{-t/\tau_i} \quad (5)$$

where n is the number of fluorophores (emitting states), the τ_i are the individual lifetimes, and the pre-exponential α_i values are weighting terms that depend on each fluorophore's concentration, extinction coefficient at the excitation wavelength, and emission spectrum, as well as the detection wavelength and bandpass. In the following derivation, it is assumed that n intensity decay lifetimes result from n different *non-interacting* excited states and that each excited state decays with single exponential kinetics.

Each of the n fluorophores has its own distinct anisotropy function, $r_i(t)$. Consequently, the decays observed at the

other two emission polarizer angles become

$$I_V(t) = \frac{1}{3}\sum_{i=1}^{n} \alpha_i\, e^{-t/\tau_i}\{1 + 2r_i(t)\} \quad (6)$$

$$I_H(t) = \frac{1}{3}\sum_{i=1}^{n} \alpha_i\, e^{-t/\tau_i}\{1 - r_i(t)\} \quad (7)$$

with $r_i(t)$ defined as:

$$r_i(t) = \sum_{j=1}^{m_i} \beta_{ij}\, e^{-t/\phi_{ij}} \quad (8)$$

where ϕ_{ij} is the jth correlation time for the ith fluorophore. The m_i are the number of correlation times for each of the n fluorophores and, along with β_{ij} and ϕ_{ij}, may be different for each fluorophore.

With no loss of generality, Eq. 8 can be simplified as follows:

$$r_i(t) = \sum_{j=1}^{m} \beta_{ij}\, e^{-t/\phi_j} \quad (9)$$

By listing the correlation times in a one-dimensional array, Eq. 9 frequently is a simplification because each correlation time is not unique to a single fluorophore. For example, all fluorophores attached to a macromolecule will have common correlation times as a result of the rotational motions of the macromolecule. Thus, the number of decay parameters to be determined is reduced, which will help in their recovery and facilitate an understanding of the underlying physical mechanisms. Added benefits are that Eq. 9 is intuitively simpler to comprehend and only a single m value needs to be established instead of several m_i terms. Provided that n and m are known correctly, a set of β_{ij} terms can be found, using Eq. 9, which describe any possible association between the excited-state fluorophores and the depolarizing processes.

The dependence of the β_{ij} terms on both the excitation and emission dipoles stipulates that a β_{ij} depends on the identity of the excited state. If the β_{ij} terms are assumed to be the same for each fluorophore, then the expressions in Eqs. 6 and 7 reduce to the homogeneous model, which yields an averaged anisotropy that cannot account for differences in the depolarizing motions experienced by the various fluorophores. Therefore, the subscript i with the β_{ij} terms may not be omitted, as was done above for the correlation times. As stated above, the β_{ij} terms represent a mapping of the jth depolarization event onto the ith fluorescence lifetime, and therefore can be different for each lifetime component τ_i. A non-zero β_{ij} implies that the ith excited-state fluorophore is depolarized by the process(es) underlying the jth component of the anisotropy decay, while a value of zero indicates that the ith excited-state fluorophore is not depolarized by the process(es) that gives rise to the jth component of the anisotropy decay. Therefore, as will be described below, various association models can be implemented during an analysis by making specific β_{ij} terms constants equal to zero.

Substitution of Eq. 9 into Eqs. 6 and 7 expands those expressions:

$$I_V(t) = \frac{1}{3}\sum_{i=1}^{n} \alpha_i\, e^{-t/\tau_i}\left\{1 + 2\sum_{j=1}^{m} \beta_{ij}\, e^{-t/\phi_j}\right\} \quad (10)$$

$$I_H(t) = \frac{1}{3}\sum_{i=1}^{n} \alpha_i\, e^{-t/\tau_i}\left\{1 - \sum_{j=1}^{m} \beta_{ij}\, e^{-t/\phi_j}\right\} \quad (11)$$

The total anisotropy decay of a mixture of fluorophores is defined as

$$r(t) = \frac{I_V(t) - I_H(t)}{I_V(t) + 2I_H(t)} \quad (12)$$

Insertion of Eqs. 10 and 11 into Eq. 12, followed by algebraic simplifications, results in

$$r(t) = \frac{\sum_{i=1}^{n} \alpha_i\, e^{-t/\tau_i} \sum_{j=1}^{m} \beta_{ij}\, e^{-t/\phi_j}}{\sum_{i=1}^{n} \alpha_i\, e^{-t/\tau_i}} \quad (13)$$

This expression for $r(t)$ differs from that usually used (Lakowicz, 1983) in that the intensity decay elements do not cancel, reflecting the unique anisotropy decay of each individual fluorophore.

In this kinetic scheme, where each lifetime is due to a specific excited-state fluorophore, the sum of the β_{ij} for a particular lifetime component represents the limiting anisotropy, r_0, for that excited state. Therefore, the limits on acceptable values for the β_{ij} terms must be applied separately for each excited-state fluorophore. As stated above, theory limits this sum to the range $-0.2 \le r_0 \le 0.4$. As described in Materials and Methods, these constraints on the recovered β_{ij} can be used as criteria to guide the decision for accepting or rejecting a particular lifetime-correlation time association model.

The steady-state anisotropy, $\langle r \rangle$, is the anisotropy averaged over all time. Calculation of this time average by separate integration of the numerator and denominator in Eq. 13 over all time yields

$$\langle r \rangle = \frac{\sum_{i=1}^{n} \alpha_i \tau_i \sum_{j=1}^{m} \beta_{ij} \phi_j (\tau_i + \phi_j)^{-1}}{\sum_{i=1}^{n} \alpha_i \tau_i} \quad (14)$$

Thus, Eq. 14 can be used to calculate $\langle r \rangle$ from the recovered decay parameters, and this value can then be compared to the measured value of the steady-state anisotropy.

MATERIALS AND METHODS

Samples

All chemicals used were reagent grade and all experiments were performed at 20°C. A 10% alcohol suspension of horse LADH (E.C.1.1.1.1, Boehringer Mannheim, Indianapolis, IN) was dialyzed extensively against a 0.1 M sodium phosphate buffer, pH 7.3, containing 1 mM NaN_3. Following removal of undissolved protein by centrifugation, the functional properties and homogeneity of the LADH solution were evaluated by three methods. First, enzyme concentration was calculated from the optical density at 280 nm using an extinction coefficient of 3.64×10^4 M^{-1} cm^{-1} (Theorell et al., 1966). Second, enzyme activity was assayed by measuring the rate of NADH formation (Dalziel, 1957). Finally, the number of NADH binding sites was determined from the increase in NADH fluorescence as the coenzyme was titrated into a LADH solution containing 50 mM isobutyramide. The NADH concentration at the titration end point should be twice the enzyme concentration because LADH has two binding sites for NADH (Bränden et al., 1975). The assays indicated that the enzyme concentration and the number of active sites were consistent within experimental error, implying that the enzyme was fully functional and homogeneous.

Time-resolved fluorescence spectroscopy

Fluorescence decay curves were obtained by time-correlated, single-photon counting using an instrument described previously (Hasselbacher et al., 1991). Samples were excited at 295 nm with vertically polarized light, and the emission was collected through a polarizer set at the M, V, or H position (see Theory). Emission wavelengths were selected by a Jobin-Yvon monochromator (100 mm) with a bandpass of 10 nm. Decays were typically collected into 2000 channels, yielding a timing calibration of 22 ps/channel. The instrument response function (IRF), obtained by light scattering, was collected to a minimum of 100,000 counts in the peak channel, whereas the decay curves were collected to a minimum of 40,000 counts in the peak channel. The IRF and the $I_M(t)$, $I_V(t)$, and $I_H(t)$ decay curves together constitute an anisotropy data set.

Fluorescence anisotropy data sets, both experimental and synthetic (see below), were analyzed by a reconvolution procedure (Grinvald and Steinberg, 1974) using nonlinear least-squares regression (Bevington, 1969). These data sets, consisting of the decays collected at the different emission polarizer positions, were analyzed simultaneously by a global procedure (Cross and Fleming, 1984; Waxman et al., 1993). Global analyses (Knutson et al., 1983; Beechem et al., 1983) of groups of anisotropy data sets were also employed. All fits were judged by the reduced χ^2, the weighted residuals, and the autocorrelation of the residuals.

Simulations

To synthesize anisotropy data sets, a Monte Carlo algorithm was used in an analogous manner to that previously published (Chowdhury et al., 1991). Use of this procedure avoids potential problems associated with analyzing data generated using the same algorithm that was used in the analysis, and is advantageous because the noise generated by the algorithm obeys Poisson statistics and thus is analogous to photon-counting noise. An IRF was first "collected" to 100,000 counts at the peak of a Gaussian with a half-width at half-height comparable to our experimental IRF (0.15 ns). This Gaussian function was also used in the "collection" of the $I_M(t)$, $I_V(t)$, and $I_H(t)$ decay curves, each to 40,000 counts at the peak. The same number of channels and timing calibration were used as described above for the experimental data sets. When generating the $I_V(t)$ and $I_H(t)$ decays, $r_i(t)$ was calculated at the time corresponding to each intensity decay event and then used to determine the probability that the decay event could have been observed at a given polarizer position.

Synthetic data sets were analyzed "blind," in that there was no knowledge of the values of the parameters or of the association model (see Results) used to generate a data set. However, in analogy with real data, various "experimental" details about the simulations were known. For example, the synthetic data sets were to represent those collected for a protein containing two tryptophans, each with a different single exponential intensity decay and emission spectrum. In addition, families of data sets had been generated to represent decays collected as a function of emission wavelength. Finally, it was to be assumed that excitation had been at 295 nm, which implied that the β_{ij} terms had to be greater than zero (Valeur and Weber, 1977).

Based on this information, criteria were established to help identify what particular association model was used to generate a data set. Any of the following criteria was sufficient to reject an analysis as unacceptable: 1) if the normal standards of a good fit (χ^2, residuals, autocorrelation function) were not satisfied; 2) if any β_{ij} term was ≤ 0, unless the association model required $\beta_{ij} = 0$; 3) if $(\beta_{11} + \beta_{12})$ or $(\beta_{21} + \beta_{22})$ were >0.4 (see Theory); 4) if ϕ_j was greater than $\sim 10\times$ the longest τ_i, which is based on Wahl's (1979) analysis on the recovery of anisotropy decay parameters from synthetic data; 5) if ϕ_1 and ϕ_2 were within 25% of one another, which is based on our experience for recovering accurate parameters from synthetic data sets with one lifetime and two correlation times; or 6) if $\phi_2 < \phi_1$, except for models 3 and 4 (see Results).

If any of these criteria was met, then an analysis was not acceptable. Otherwise, an analysis was acceptable even if the recovered parameters did not agree with those from other analyses. At least three analyses were done for each association model, using different groups of initial values (starting guesses) for the iterated parameters. If at least one of these attempts yielded an acceptable analysis, then the association model being tested was deemed a possible generator of that data set. However, if all analysis attempts were unacceptable, then that association model was eliminated.

After all analyses were complete, the parameters and association models used to generate the data sets were revealed. The values for many of these parameters were chosen because of their similarity to those reported for LADH (Ross et al., 1981; Eftink and Jameson, 1982; Demmer et al., 1987; Eftink et al., 1987; 1994) so that there would be a basis for decisions during the analysis of the LADH data. All synthetic data sets were generated with the same lifetimes and correlation times: $\tau_1 = 4$ ns; $\tau_2 = 7$ ns; $\phi_1 = 2$ ns; and $\phi_2 = 10$ ns. For the six data sets generated by each association model but with different α_i to simulate an experiment as a function of emission wavelength, the (normalized) α_1, α_2 values were 0.05, 0.95; 0.2, 0.8; 0.4, 0.6; 0.6, 0.4; 0.8, 0.2; and 0.95, 0.05. In addition, the tryptophan with the shorter lifetime had been assigned a blue-shifted emission spectrum characteristic of a buried residue. Consequently, this Trp residue also was assumed to have a red-shifted absorption spectrum, which meant that it had a smaller r_0 for 295 nm excitation (Valeur and Weber, 1977). The specific β_{ij} terms for the various models are listed in Table 1.

RESULTS

Nine different association models can be defined for the case of $n = m = 2$; these models are diagrammed in Fig. 1. The most general case, where each lifetime associates with each correlation time, has been designated model 0. It is difficult to envision a simple experimental test case for some of the other models. An example for models 1 and 2 would include a mixture of a fluorophore free in solution and bound rigidly to a macromolecule, with the two forms having measurably different lifetimes. Models 3 and 4 can be thought of as situations where one fluorophore is attached rigidly to such a large macromolecule that the excited state of the fluorophore decays before any appreciable rotational motion by the macromolecule. Models 6 and 7

TABLE 1 Values of the β_{ij} terms used to generate the synthetic data sets

	Association Model Used for Generation								
	Model 0	Model 1	Model 2	Model 3	Model 4	Model 5	Model 6	Model 7	Model 8
β_{11}	0.05	0.20	0.00	0.05	0.00	0.05	0.05	0.00	0.20
β_{12}	0.15	0.00	0.20	0.15	0.00	0.15	0.15	0.20	0.00
β_{21}	0.05	0.00	0.25	0.00	0.05	0.25	0.00	0.05	0.05
β_{22}	0.20	0.25	0.00	0.00	0.20	0.00	0.25	0.20	0.20

represent those situations where only one of the two fluorophores experiences depolarizing motions independent of the entire macromolecule. Models 5 and 8 can result if two fluorophores are attached rigidly to a highly asymmetric macromolecule, the rotation of which yields two unique correlation times. If the emission dipole of one fluorophore is oriented parallel to one of the macromolecule's rotation axes, this fluorophore is not depolarized by rotation about this axis. Clearly, some of these models represent unusual situations, but all were included in this study to make it comprehensive for the case of $n = m = 2$. To test whether these nine models can be discriminated from one another, they were used in the analysis of a series of synthetic data sets and were also applied to LADH data sets.

Analysis of simulated data sets

Nine families of data sets were generated, each by a different association model (Fig. 1). Each family consisted of six different anisotropy data sets representing decays collected at different emission wavelengths; see Materials and Methods for details. Each of these 54 data sets was then analyzed by all nine association models to identify, if possible, which model generated which data set.

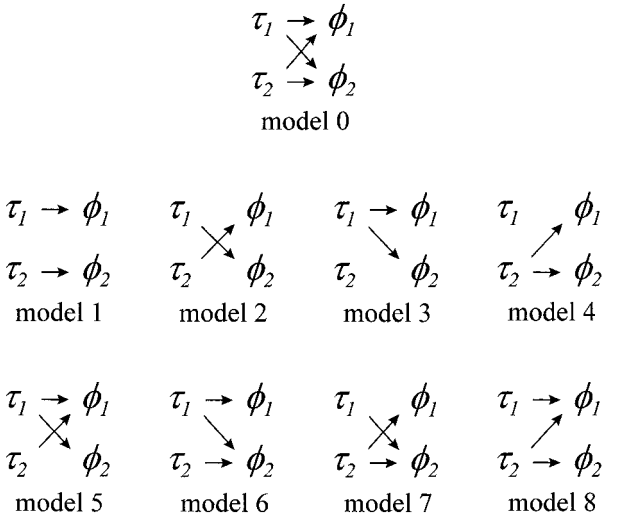

FIGURE 1 The nine possible fluorescence intensity lifetime-rotational correlation time association models for $n = m = 2$. In the analyses using these models it is necessary to adopt a consistent ordering based on magnitudes. Consequently, for this work $\tau_1 < \tau_2$ and $\phi_1 < \phi_2$.

To help assess the results from all of the analyses, the 54 data sets were sorted into six groups based on the normalized recovered values for α_1 and α_2. As an example, the results for the group of data sets yielding $\alpha_1 \approx 0.4$ and $\alpha_2 \approx 0.6$ are given in Table 2, from which it is apparent that some models yielded more acceptable analyses than others when applied to the nine data sets. Interestingly, all nine models provided acceptable analyses of data set *ix*. The number of acceptable analyses in the various groups was dependent on the ratio of the α_i terms. As indicated in Fig. 2, there were fewer acceptable analyses for data sets with small α_i values. Thus, the ability of the decay parameters to accommodate the different kinetic schemes decreases as the contribution of one lifetime component to the total fluorescence becomes small.

Using these six groups of data sets, an attempt was made to reason which model generated which data set. Because all of the data sets in Table 2 could be analyzed acceptably by at least six of the models, no assignment of a specific model to a particular data set can be rationalized. A similar inability to resolve the generation models was found for the other five α_1-, α_2-related groups (not shown). In fact, the result of analyzing all synthetic data sets individually by all nine association models was the assignment of a model to only three data sets. [It might be argued that additional assignments are possible. For example, data set *ix* in Table 2 might have been generated by model 3 because it was the only data set that model 3 could analyze. This assumes, however, that each data set in Table 2 had been generated by a

TABLE 2 Individual analyses of data sets with $\alpha_1 \approx 0.4$ and $\alpha_2 \approx 0.6$

Data Set	Association Model Used for Analysis								
	0	1	2	3	4	5	6	7	8
i	o	o	x	x	o	x	o	o	o
ii	o	o	x	x	o	x	o	o	o
iii	o	o	x	x	o	x	o	o	o
iv	o	o	o	x	o	o	x	o	o
v	o	o	x	x	o	x	o	o	o
vi	o	o	x	x	o	x	o	o	o
vii	o	o	o	x	o	o	x	o	o
viii	o	o	x	x	o	x	o	o	o
ix	o	o	o	o	o	o	o	o	o

Analyses of these nine data sets (*i–ix*) yielded equivalent normalized intensity decay pre-exponential terms. An "o" or "x" denotes an acceptable or unacceptable analysis, respectively, based on the criteria listed in Materials and Methods.

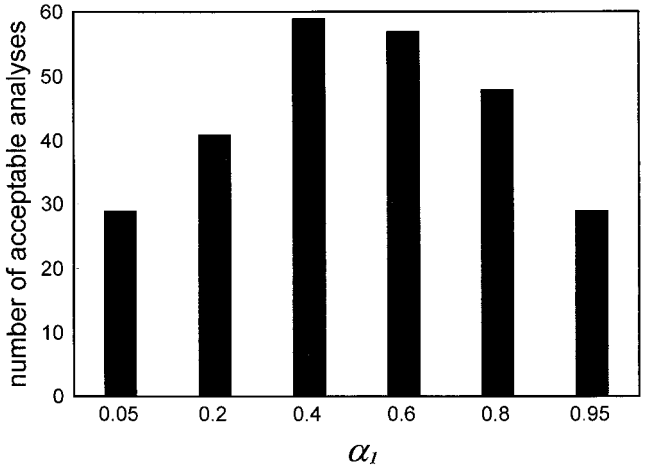

FIGURE 2 The number of acceptable individual analyses for the 54 synthetic data sets as a function of the normalized value for α_1, with $\alpha_2 = 1 - \alpha_1$. For example, there are 59 "o" entries for the group of data sets in Table 2 where $\alpha_1 = 0.4$.

different model, information which is not known for an experimental system. Consequently, this reasoning was not applied here.] It was therefore concluded that the analysis of individual anisotropy data sets was not sufficient to discriminate among the various models. The validity of this conclusion was confirmed when the generation models and parameters were revealed (see below), and it was found that all three assignments were incorrect. Interestingly, these three assignments were in the two groups containing data sets generated with an $\alpha_i = 0.05$.

As the next step toward identification of the generation models, the six data sets in each of the nine families were analyzed simultaneously, in a global procedure (Knutson et al., 1983; Beechem et al., 1983), by each of the nine association models. This procedure was appropriate because the families had been generated to represent an actual experimental system examined at different emission wavelengths. The placement of a data set within one of the nine families (A–I) was done without revealing the identity of its generation model, which was specific to that family. Various parameters, such as the intensity decay lifetimes and the rotational correlation times, were made common to all six data sets within a family in an attempt to constrain the analyses sufficiently so as to permit discrimination among the association models. The rejection criteria were the same as for the analysis of the individual data sets; these criteria were evaluated individually for each data set within a family, and all data sets had to satisfy them for the global analysis to be considered acceptable. The trend in the steady-state anisotropies calculated from the iterated parameters (Eq. 14) was also monitored because they should have a monotonic trend related to the changing intensity decay amplitudes.

When only the lifetimes were made common, no improvement in the ability to discriminate among the models was noted. However, if the correlation times were included as common parameters, the effect of the additional constraints was striking. As shown in Table 3, only a single model was acceptable for six of the families (A, C, D, E, F, and G), and it was a different model for each family. No model met all of the analysis criteria for the other three families (B, H, and I). However, for each of these families there was one model, indicated by the ⊗ in Table 3, that stood out as being nearly acceptable. Again, it was a different model for each family. Models 0, 5, and 8 failed for families B, I, and H, respectively, only because the value of β_{11} was negative or too large for those data sets generated with α_1 equal to either 0.05 or 0.2. Thus, these global analyses yielded a unique assignment of a single, different association model to six of the families and a possible assignment for the other three families.

Additional analyses were performed on families B, H, and I in which the β_{ij} were also made common to all six data sets. Global analyses of family B by all nine models, with all τ_i, ϕ_j, and β_{ij} terms common, confirmed the tentative assignment made in the previous round of analyses: only model 0 met all criteria for an acceptable analysis. Similar global analyses performed on families H and I also confirmed their tentative assignment to a generation model: families H and I were probably generated by models 8 and 5, respectively. Following this series of global analyses, the generation codes and parameters were revealed and the assignments of association models to the families of data sets were in fact correct.

Two interesting results were obtained from the global analyses when all the τ_i, ϕ_j, and β_{ij} terms were made common. First, an analysis of families H and I by model 0 was sufficient to deduce the generation model. In both cases, the appropriate β_{ij} term iterated to zero: β_{12} for family H indicating model 8 and β_{22} for family I denoting model 5. To evaluate the generality of this result, the remaining families were re-analyzed by model 0 with the β_{ij} terms included as common parameters. In all cases, the appropriate β_{ij} term for the model and data set family iterated to zero. Second, as the number of common parameters increased, all iterated parameters were recovered with

TABLE 3 Global analyses of the nine synthetic data set families

Data Set Family	Association Model Used for Analysis								
	0	1	2	3	4	5	6	7	8
A	x	x	x	x	x	x	x	O	x
B	⊗	x	x	x	x	x	x	x	x
C	x	x	x	x	x	x	O	x	x
D	x	O	x	x	x	x	x	x	x
E	x	x	O	x	x	x	x	x	x
F	x	x	x	x	O	x	x	x	x
G	x	x	x	O	x	x	x	x	x
H	x	x	x	x	x	x	x	x	⊗
I	x	x	x	x	x	⊗	x	x	x

An "O" or "x" denotes an acceptable or unacceptable analysis, respectively, as determined by the criteria listed in Materials and Methods. See the text for an explanation of the ⊗ symbol.

greater accuracy. This effect was especially pronounced when the β_{ij} terms were included as common parameters.

Analysis of LADH data sets

Because the two tryptophan residues per subunit of LADH have different emission spectra (Laws and Shore, 1978), anisotropy data sets were obtained between 310 and 380 nm in 10-nm intervals. Because both lifetimes must associate with the long correlation time, global analyses of these data sets focused on association models 0, 6, and 7 (Fig. 1). [Note: test analyses with the other six models all yielded unacceptable results.] All of the τ_i, ϕ_j, and β_{ij} terms were common parameters and the same rejection criteria that were applied to the analyses of the simulations were employed. Analysis of these data sets clearly indicated that only model 6 was acceptable; the values of the recovered parameters are given in Table 4. The two lifetimes of near 4 and 7 ns agree with those previously found for LADH protein fluorescence (Ross et al., 1981; Eftink and Jameson, 1982; Demmer et al., 1987; Eftink et al., 1987; 1994). The α_i terms indicate that the intensity of the Trp residue with the shorter lifetime dominates at the blue side of the emission spectra, and their values at 310 and 320 nm approach the extremes of the α_i used in the simulations. Inclusion of the 310 and 320 nm data sets was crucial for the determination of a model because poor fit statistics for these two data sets were the decisive factors for the rejection of model 7.

DISCUSSION

Recovery of accurate information about a biological system, especially with respect to the localization of dynamic processes to specific fluorophores, requires kinetic parameters defining the unique intensity and anisotropy decays of *each* fluorophore. Therefore, this study presents a kinetic scheme that permits an evaluation of the intensity and anisotropy decay parameters for each fluorophore. All possible association models, specifying how each lifetime component maps into each anisotropy component, are defined through a unique set of β_{ij} terms.

This kinetic scheme can be applied to many of the biomolecular systems for which the fluorescence is characterized by multiple lifetimes and correlation times. These systems would include those in which multiple fluorescence lifetimes arise from multiple fluorophores or multiple environments for a single fluorophore. In addition, it accounts for those situations where multiple correlation times arise from asymmetric macromolecules and/or local motions within a macromolecule or its complexes. There are certain situations, however, where this kinetic scheme is inappropriate. When multiple fluorescence lifetimes arise from processes occurring during the excited state, then distinct associations between lifetimes and correlation times cannot be made because the observed lifetimes are complex functions of all rate constants. There may also be situations where this kinetic scheme can in principle describe the anisotropy decay, but where application of these models would be problematic. For example, consider a macromolecular assembly reaction in which the lifetime of a single fluorophore is the same for all of the various species. A naive analysis of the anisotropy decay of such a system would recover one lifetime and multiple correlation times, but with β terms that would be functions of the populations of the various assembly states. As a result of this incorrect approach to the analysis, the number of correlation times and their values also might be in error. To recover pertinent information for *each* of the various states of the macromolecule, the analysis must be forced to accommodate the fact that each species has a unique lifetime, τ_i, even though the value of this lifetime is the same for all species. Importantly, the corresponding α_i term represents the relative concentration of that species. Explicit α_i terms can be applied to an analysis from knowledge of the equilibrium concentrations previously established for each species by another technique. By applying this constraint, the fluorescence intensity contribution from each state of the macromolecule is established, which enhances the chances of recovering the proper anisotropy parameters. Thus, even in this complicated situation, the present kinetic scheme could provide hydrodynamic and local dynamic information about each form of the macromolecule.

The general form of the anisotropy decay for multiple fluorophores developed here requires resolution of a significantly greater number of kinetic parameters than for the decay of a single fluorophore, especially because each fluorophore may have several depolarizing motions. The number of kinetic parameters, and the statistical correlations between them, is the most likely reason that the individual analyses of the two-lifetime, two-correlation time synthetic data sets were unable to accurately recover the association model or the values of the parameters used for generation.

The improvement obtained by the global analyses clearly demonstrates that to make distinctions between the association models it is necessary to constrain the search for the parameters. Thus, additional information about the system

TABLE 4 LADH fluorescence decay parameters recovered by association model 6

Common Parameters								
	τ_1 (ns)	τ_2 (ns)	ϕ_1 (ns)	ϕ_2 (ns)	β_{11}	β_{12}	β_{21}	β_{22}
	3.9	7	1.7	42	0.028	0.201	0	0.193
Independent Parameters								
	Wavelength (nm)							
α_i*	310	320	330	340	350	360	370	380
α_1	0.89	0.85	0.77	0.73	0.68	0.63	0.59	0.55
α_2	0.11	0.15	0.23	0.27	0.32	0.37	0.41	0.45

*Normalized to a sum of one.

under study is required. Increasing the number of common parameters increases the chance of determining the correct association model as well as recovering accurate decay parameters. As a result, the ability to resolve the applicable association model was enhanced markedly not only for the synthetic, but also for the LADH data sets.

Two other salient points are demonstrated by the results of the global analyses of the synthetic data sets. First, to resolve the correct associations between lifetimes and correlation times in an experimental system, it is important to obtain data sets over the maximum available range of the independent variable. The need for a wide range of values is apparent from the effect on the global analyses of the synthetic data sets when increasing the number of common parameters. For example, consider models 0, 5, and 8, which are the only models where both lifetimes are associated with the short correlation time, ϕ_1. When only lifetimes and correlation times were common to each data set, analyses failed for these models because of an unacceptable value for β_{11} in the data sets where there was a minor contribution to the total fluorescence intensity from the short lifetime, τ_1. When the β_{ij} terms were included as common parameters, those data sets with an appreciable intensity contribution from the short lifetime component were able to constrain the β_{11} term appropriately and permit recovery of the correct β_{11} term. Consequently, these data sets with a small contribution from one lifetime component played an essential role in confirming the appropriate association model. Second, and perhaps most importantly, the present application of global analysis to fluorescence data has proved useful for discriminating between a group of similar physical models.

Intrinsic LADH fluorescence excited at 295 nm is from the two tryptophan residues, Trp-15 and Trp-314, per subunit of the homodimeric enzyme. Previous studies have established that the fluorescence of each residue decays with a single, distinct lifetime (Ross et al., 1981; Eftink and Jameson, 1982; Demmer et al., 1987; Eftink et al., 1987; 1994). Eftink et al. (1994) reported the need for two correlation times in their analysis of the fluorescence anisotropy decay of LADH. These authors, however, were unable to report a specific value for the short correlation time or determine whether only one or both Trp residues were subject to a rapid depolarization event. Our preliminary report (Bialik et al., 1998) suggested that only Trp-15 was involved, but this conclusion was not definitive because it was based on data recorded over a narrow range of emission wavelengths. The present results agree that only one tryptophan undergoes the rapid depolarizing process(es), but indicate that the short correlation time is associated with the residue having the 4-ns lifetime, which is Trp-314 (Ross et al., 1981; Eftink and Jameson, 1982; Demmer et al., 1987; Eftink et al., 1987; 1994). It is difficult to understand, however, how Trp-314 is capable of local depolarizing motions, because it is buried at the subunit interface with essentially no adjacent free space (Bränden et al., 1975). In fact, the x-ray crystallography B values reported for the LADH ternary complex with NADH and DMSO imply a highly ordered, rigid interface between the subunits (Al-Karadaghi and Cedergren-Zeppezauer, personal communication; Bernstein et al., 1977; Abola et al., 1987). By contrast, Trp-15 might have been expected to undergo a local depolarizing motion because it is on the surface of the enzyme, a hypothesis that can only be rejected by means of the analysis procedures developed here.

Other possible depolarizing mechanisms must be considered given that Trp-314 appears highly constrained and unlikely to exhibit significant local motions. One depolarizing mechanism not requiring any local motion would be resonance energy transfer from Trp-314 in one subunit to Trp-314 in the other subunit. [For a discussion of depolarization by resonance energy transfer, see Förster, 1948.] Examination of the LADH structure shows that the centers of mass for the two Trp-314 indole rings are within 7 Å of one another (Al-Karadaghi and Cedergren-Zeppezauer, personal communication; Bernstein et al., 1977; Abola et al., 1987). In addition, because these two tryptophans have red-shifted absorption and blue-shifted emission spectra, they should have an appreciable overlap of isoenergetic states. If resonance energy transfer does occur, some depolarization would be expected because the indole ring of one residue is at an angle with respect to the indole ring of the other. The small value for β_{11} (Table 4) is consistent with this possible mechanism.

Invoking a mechanism other than local dynamics to explain the independent depolarization of Trp-314 in LADH implies that the kinetic schemes diagrammed in Fig. 1 may be inappropriate. Consequently, although statistically acceptable fits to the data were obtained, it is conceivable that an inappropriate kinetic scheme has been found acceptable and that certain parameters were not recovered with physically accurate values. Two factors suggest either that incorrect assumptions have been made about the Trp residues in LADH or that the present data analysis by model 6 is not sufficient. First, the relative values of the limiting anisotropies for the two Trp residues are not what would be expected. Because the shorter lifetime species also has the more blue emission, it should have the more red excitation and thus the smaller r_0. Instead, the model 6 analysis yields an r_0 value of 0.229 ($\beta_{11} + \beta_{12}$, Table 4) for the Trp residue with the shorter lifetime, whereas the r_0 value for the longer lifetime Trp residue is 0.193. Second, the recovered value of 42 ns for ϕ_2 is 5–10 ns longer than expected from a calculation (Waxman et al., 1993) assuming that LADH is a hydrated sphere of mass 80,000 Da. Regardless of whether the association models in Fig. 1 can describe depolarization by resonance energy transfer, the present results infer that the depolarizing mechanism(s) underlying the rapid component of the anisotropy decay is experienced only by Trp-314. The LADH studies are being continued to clarify these issues and, hopefully, the appropriate depolarizing mechanism underlying the anisotropy decay will be identified.

In summary, the analysis of time-resolved fluorescence anisotropy data by global analysis using association models

TABLE 5 Number of possible associations between lifetimes and correlation times

	n			
m	1	2	3	4
1	1	3	7	15
2	1	9	49	225
3	1	27	343	3375
4	1	81	2401	50625

Calculated by $(2^n - 1)^m$, where n and m are the number of lifetimes and correlation times, respectively.

has great potential for providing structural information on biological macromolecules in solution as well as for evaluating rapid local and segmental dynamic motions. It might therefore be possible, for example, to resolve not only the rotational correlation times for a biomolecule whose overall shape resembles an ellipsoid, but also the independent depolarizing motions of the multiple fluorophores associated with that biomolecule.

To facilitate the use of this general kinetic scheme, more studies are needed to verify its versatility. For example, more tests even for the relatively simple case when $n = m = 2$ are required, especially performing simulations over a wider range of parameter values to help establish limitations that this analysis approach might have. In addition, more experimental systems need to be evaluated. Further advancement of this approach, in terms of both simulations and experimental studies, will come from examining systems characterized by more than two lifetimes and correlation times. As noted in Table 5, however, the number of possible associations increases rapidly. Simulations should reveal the feasibility of determining the correct association model for a given number of lifetimes and correlation times, and a set of parameter values. A potential simplification arises from the observation that an analysis by model 0 for the $n = m = 2$ simulations was able to reveal the appropriate association model *provided adequate constraints were placed on the analysis*. Consequently, a "model 0" analysis for each set of n and m might be sufficient to reveal the appropriate model. Even if a single model is not indicated, a model 0 analysis might facilitate the elimination of a large subset of related association models, and thus minimize the number of specific models that must be tested. Physical arguments also can be used to reject certain models. For instance, as mentioned previously, if all fluorophores in a sample are bound to a single macromolecule, they all must be depolarized in part by the same rotational motions. Combining the power of physical arguments with global analyses of large scale experiments should help in the assignment of complex depolarizing dynamics to specific macromolecular domains. As demonstrated by the results with LADH, the mechanistic interpretation of these localized dynamics can increase the understanding of the fundamental properties of a macromolecule.

This work has been supported in part by National Institutes of Health Grants GM39750 and HL29019. Support for ELR came from National Institutes of Health Grant CA63317.

REFERENCES

Abola, E. E., F. C. Bernstein, S. H. Bryant, T. E. Koetzle, and J. Weng. 1987. Protein data bank. *In* Crystallographic Databases—Information Content, Software Systems, Scientific Applications. F. H. Allen, G. Bergerhoff, and R. Sievers, editors. Data Commission of the International Union of Crystallography, Bonn/Cambridge/Chester. 107–132.

Azumi, T., and S. P. McGlynn. 1962. Polarization of the luminescence of phenanthrene. *J. Chem. Phys*. 37:2413–2420.

Badea, M., and L. Brand. 1979. Time-resolved fluorescence measurements. *Methods Enzymol*. 61:378–425.

Beechem, J. M., J. R. Knutson, J. B. A. Ross, B. W. Turner, and L. Brand. 1983. Global resolution of heterogeneous decay by phase/modulation fluorometry: mixtures and proteins. *Biochemistry*. 22:6054–6058.

Bernstein, F. C., T. F. Koetzle, G. J. B. Williams, E. F. Meyer, Jr., M. D. Brice, J. R. Rodgers, O. Kennard, T. Shimanouchi, and M. Tasumi. 1977. The protein data bank: a computer-based archival file for macromolecular structures. *J. Mol. Biol*. 112:535–542.

Bevington, P. R. 1969. Data Reduction and Error Analysis for the Physical Sciences. McGraw-Hill, New York. 204–246.

Bialik, C. N., B. Wolf, E. L. Rachofsky, J. B. A. Ross, and W. R. Laws. 1998. Fluorescence anisotropy decay: finding the correct physical model. *SPIE*. 3256:60–67.

Bialik, C., B. Wolf, J. B. A. Ross, and W. R. Laws. 1997. Analysis of fluorescence anisotropy decay: specific associations between lifetimes and rotational correlation times. *Biophys. J*. 72:89*a*. (Abstr.).

Brand, L., J. R. Knutson, L. Davenport, J. M. Beechem, R. E. Dale, D. G. Walbridge, and A. A. Kowalczyk. 1985. Time-resolved fluorescence spectroscopy: some applications of associative behaviour to studies of proteins and membranes. *In* Spectroscopy and the Dynamics of Molecular Biological Systems. P. M. Bayley and R. E. Dale, editors. Academic Press, London. 259–305.

Bränden, C.-I., H. Jornvall, H. Eklund, and B. Furugren. 1975. Alcohol dehydrogenases. *In* The Enzymes. P. D. Boyer, editor. Academic Press, New York. 103–190.

Chowdhury, F. N., Z. S. Kolber, and M. D. Barkley. 1991. Monte Carlo convolution method for simulation and analysis of fluorescence decay data. *Rev. Sci. Instrum.* 62:47–52.

Chuang, T. J., and K. B. Eisenthal. 1972. Theory of fluorescence depolarization by anisotropic rotational diffusion. *J. Chem. Phys*. 57: 5094–5097.

Cross, A. J., and G. R. Fleming. 1984. Analysis of time-resolved fluorescence anisotropy decays. *Biophys. J*. 46:45–56.

Dalziel, K. 1957. Assay and specific activity of crystalline alcohol dehydrogenase of horse liver. *Acta Chem. Scand*. 11:397–398.

Demmer, D. R., D. R. James, R. P. Steer, and R. E. Verrall. 1987. Three exponential fluorescence decay of horse liver alcohol dehydrogenase revealed by iodide quenching. *Photochem. Photobiol*. 45:39–48.

Eftink, M. R., and D. M. Jameson. 1982. Acrylamide and oxygen fluorescence quenching studies with liver alcohol dehydrogenase using steady-state and phase fluorometry. *Biochemistry*. 21:4443–4449.

Eftink, M. R., Z. Wasylewski, and C. A. Ghiron. 1987. Phase-resolved spectral measurements with several two tryptophan containing proteins. *Biochemistry*. 26:8338–8346.

Eftink, M. R., C.-Y. Wong, D.-H. Park, G. L. Shearer, and B. V. Plapp. 1994. Comparison of fluorescence properties of wild types and the W15F mutant of horse liver alcohol dehydrogenase. *SPIE*. 2137: 120–126.

Förster, Th. 1948. Intermolecular energy migration and fluorescence. *Ann. Phys. (Leipzig)*. 2:55–75.

Grinvald, A., and I. Z. Steinberg. 1974. On the analysis of fluorescence decay kinetics by the method of least squares. *Anal. Biochem*. 59: 583–598.

Hasselbacher, C. A., E. Waxman, L. T. Galati, P. B. Contino, J. B. A. Ross, and W. R. Laws. 1991. Investigation of hydrogen bonding and proton

transfer of aromatic alcohols in nonaqueous solvents by steady-state and time-resolved fluorescence. *J. Phys. Chem*. 95:2995–3005.

Kalantar, A. H. 1968. Consequences of photoselection on the intensity and polarization of luminescent molecules. *J. Chem. Phys*. 48:4992–4996.

Kinosita, Jr., K., A. Ikegami, and S. Kawato. 1982. On the wobbling-in-cone analysis of fluorescence anisotropy decay. *Biophys. J*. 37:461–464.

Knutson, J. R., J. M. Beechem, and L. Brand. 1983. Simultaneous analysis of multiple fluorescence decay curves: a global approach. *Chem. Phys. Lett*. 102:501–507.

Lakowicz, J. R. 1983. Principles of Fluorescence Spectroscopy. Plenum Press, New York.

Laws, W. R., and J. D. Shore. 1978. The mechanism of quenching of liver alcohol dehydrogenase fluorescence due to ternary complex formation. *J. Biol. Chem*. 253:8593–8597.

Paoletti, J., and J.-B. LePecq. 1969. Correction for instrumental errors in measurement of fluorescence and polarization of fluorescence. *Anal. Biochem*. 31:33–41.

Restall, C. J., R. E. Dale, E. K. Murray, C. W. Gilbert, and D. Chapman. 1989. Rotational diffusion of calcium-dependent adenosine-5′-triphosphatase in sarcoplasmic reticulum: a detailed study. *Biochemistry*. 23:6765–6776.

Ross, J. B. A., C. J. Schmidt, and L. Brand. 1981. Time-resolved fluorescence of the two tryptophans in horse liver alcohol dehydrogenase. *Biochemistry*. 20:4369–4377.

Shinitzky, M. 1972. Effect of fluorescence polarization on fluorescence intensity and decay measurements. *J. Chem. Phys*. 56:5979–5981.

Small, E. W., and I. Isenberg. 1977. Hydrodynamic properties of a rigid molecule: rotational and linear diffusion and fluorescence anisotropy. *Biopolymers*. 16:1907–1928.

Stein, R. A., R. D. Ludescher, P. S. Dahlberg, P. G. Fajer, R. L. H. Bennett, and D. D. Thomas. 1990. Time-resolved rotational dynamics of phosphorescent-labeled myosin heads in contracting muscle fibers. *Biochemistry*. 29:10023–10031.

Theorell, H., S. Taniguchi, A. Akeson, and L. Skursky. 1966. Crystallization of a separate steroid-active liver alcohol dehydrogenase. *Biochem. Biophys. Res. Commun*. 24:603–610.

Valeur, B., and G. Weber. 1977. Resolution of the fluorescence excitation spectrum of indole into the ^1L_a and ^1L_b excitation bands. *Photochem. Photobiol*. 25:441–444.

Van der Heide, U. A., M. A. M. J. Zandvoort, E. van Faassen, G. van Ginkel, and Y. K. Levine. 1993. On the interpretation of fluorescence anisotropy decays from probe molecules in lipid vesicle systems. *J. Fluorescence*. 3:271–279.

Vogel, H., and F. Jaehnig. 1984. Fast and slow orientational fluctuations in membranes. *Proc. Natl. Acad. Sci. USA*. 82:2029–2033.

Wahl, Ph. 1979. Analysis of fluorescence anisotropy decays by a least squares method. *Biophys. Chem*. 10:91–104.

Waxman, E., W. R. Laws, T. M. Laue, Y. Nemerson, and J. B. A. Ross. 1993. Human factor VIIa and its complex with soluble tissue factor: evaluation of asymmetry and conformational dynamics by ultracentrifugation and fluorescence anisotropy decay methods. *Biochemistry*. 32:3005–3012.